

Contents	Page
The Urban Heat Island Effect in Japan's Major Cities	1
Summary of Kosa (Aeolian dust) Events over Japan in 2011	3
Sea Ice in the Sea of Okhotsk for the 2010/2011 Winter Season	4
JMA's New Climatological Normals for Atmospheric Circulation Fields	5
The GFCS at the Sixteenth World Meteorological Congress	6
Introduction of New Services Available on the TCC Website	7
TCC and GPC Tokyo's Introduction as Operational DCPCs for the WMO Information System (WIS)	8
New Head of the Tokyo Climate Center	8

The Urban Heat Island Effect in Japan's Major Cities

Ever since modern cities began to develop in the early 20th century, urban dwellers have experienced increasingly warmer climates than their contemporaries living in rural surroundings. Figure 1 shows long-term changes in annual mean air temperatures observed in the major Japanese cities of Tokyo, Sapporo, Nagoya, Osaka and Fukuoka compared

with temperatures at non-urban stations, as well as sea surface temperatures in the waters surrounding the country. Roughly speaking, non-urban station temperature records indicate a trend rising at a rate of around 1°C per century, largely reflecting global warming caused by increased atmospheric concentration of greenhouse gases. In contrast,

urban temperatures show warming at a significantly higher rate, especially in Tokyo, where the annual mean temperature has risen at more than 3°C per century. The striking departure in the long-term rate of warming in major cities from that of non-urban areas arises from the gradually intensifying urban heat island (UHI) effect. In the temperate moist climate zone of the Japanese mainland, pristine land surfaces are typically covered with rich vegetation. Grassland or forests in their natural conditions have the capacity to hold large amounts of moisture, which is released with latent heat into the upper atmosphere through evaporation and transpiration on days when strong summer sunlight parches the ground, thereby moderating land surface temperatures. However, in modern developed cities such as Tokyo, houses, buildings, paved roadways, and other human-made infrastructural

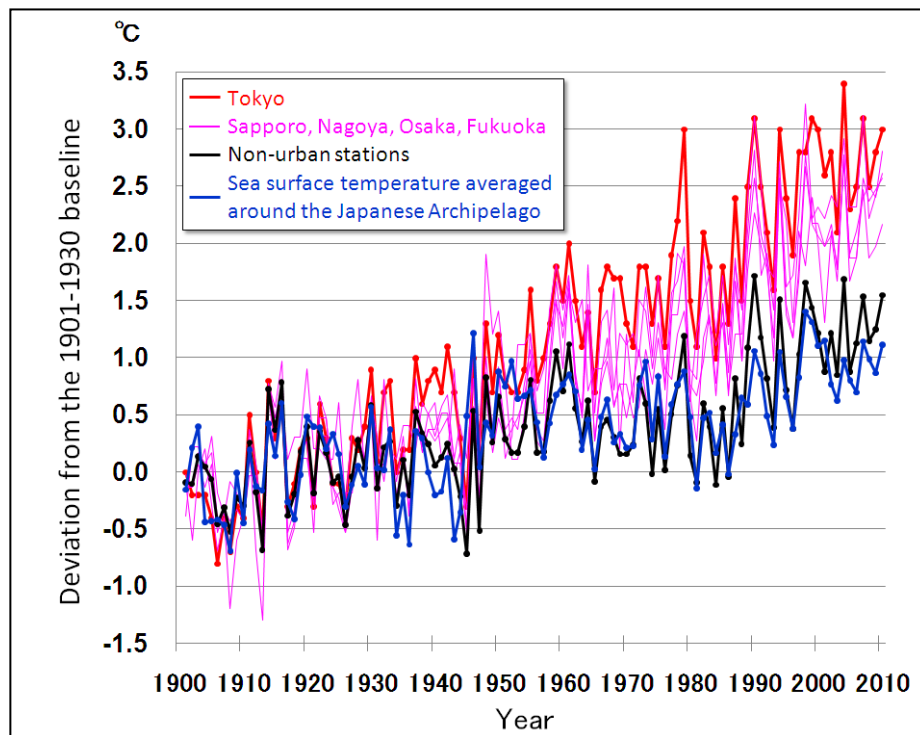


Figure 1 Long-term changes in annual mean surface air temperatures recorded at urban stations in Tokyo (the thick red line), Sapporo, Nagoya, Osaka and Fukuoka (the thin pink lines)

Temperatures averaged across non-urban stations (the black line) along with sea surface temperatures in the waters surrounding Japan (the blue line) are also shown for comparison. Each sequence of temperatures is presented as the deviation from the 1901 – 1930 average.

elements proliferate in a way that gradually encroaches upon vegetation. On dry, impermeable and lifeless urban surfaces with little vegetation left, the natural cooling thermostat based on evaporation and transpiration ceases to work.

During the night, the high-rise buildings that pack city centers impede cooling caused by the emission of infrared radiation into space because of the reduced portion of open sky viewable from a given point on an urban surface. This increased urban canopy roughness reduces the passage of wind, leading to lower efficiency in the upward turbulent diffusion of near-surface heat. Additionally, anthropogenic heat emitted from air-conditioners, automobiles and other equipment that consumes energy cannot be underestimated in highly populated city centers. These factors are all known to contribute in varying degrees to the formation of UHI.

Given that UHI is a climatological phenomenon whose effects are seen on a spatially limited scale of perhaps less than 100 km, it is obviously beyond the scope of the existing meteorological observation network to fully capture the effect's spatial structure and evolution over time. The Japan

Meteorological Agency (JMA) operates a numerical urban climate model (UCM) that can resolve the atmosphere into 4-km horizontal grids to allow investigation of how UHI evolves in Japan's metropolitan regions and measurement of the extent to which the phenomenon accounts for higher urban temperatures. Climate model simulation makes it possible to reproduce temperatures under actual urban ground conditions as well as to estimate how the climate might be under hypothetical ground conditions with no influence from urbanization. Comparing the results of hypothetical non-urban simulations with those of realistic urban simulations produces a clear picture of UHI's characteristics.

On 17 August, 2010, the temperature soared to 37.2°C according to the thermometer at the station of JMA's headquarters in Tokyo. This was the highest temperature of the summer, which in turn proved to be the hottest season in more than a century of climate records. The results of UCM simulations for that day are shown in Figure 2. The urban simulation with actual ground boundary conditions reproduces high surface air temperatures exceeding 35°C

from the coast of Tokyo Bay toward the inland area of the Kanto Plain (Figure 2 (a)). The non-urban simulation with ground boundary conditions replaced by hypothetical pristine grassland provides reference temperatures for comparison (not shown). Subtracting the non-urban temperatures from the urban temperatures on a grid-by-grid basis produces a snapshot of UHI intensity (Figure 2 (b)).

It is notable that the peak UHI intensity, which is larger than +3°C, does not appear in the most densely populated area along the coast of Tokyo Bay, but instead tends to sprawl further inland. The landward shift of the peak UHI appearance indicates that the relatively cool sea breeze from Tokyo Bay is hampered from reaching inland areas by increased surface roughness and a well-developed vertical mixed layer over central Tokyo (Figure 2 (c)).

*(Yoshinori Oikawa,
Climate Prediction Division)*

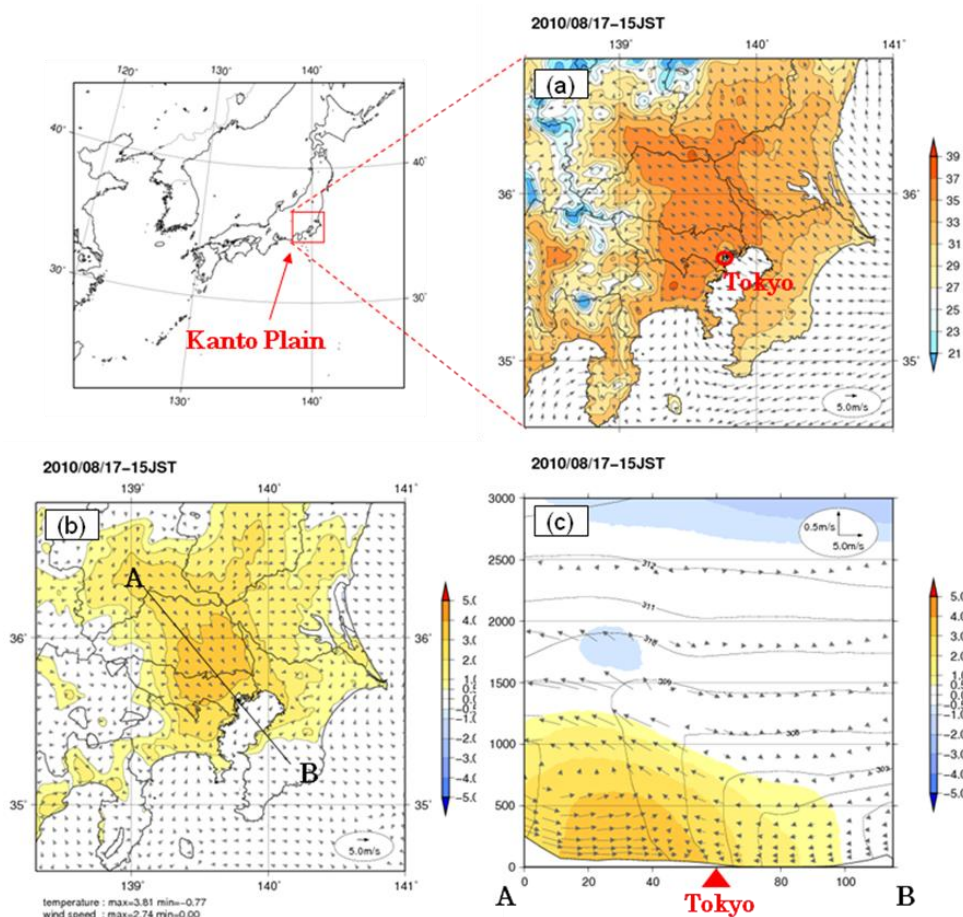


Figure 2

(a) Surface air temperatures over the Kanto Plain at 3 p.m. on 17 August 2010, as reproduced by a UCM simulation

(b) UHI intensity defined as temperature differences between the urban simulation and the hypothetical non-urban simulation

(c) UHI intensity in a northwest-southeast vertical section across the line segment connecting Point A through the center of Tokyo to Point B (shown in Map (b))

The arrows represent wind velocity differences between the urban simulation and the non-urban simulation. The contours indicate potential temperatures.

Summary of Kosa (Aeolian dust) Events over Japan in 2011

Characteristics of Kosa events in 2011

From January – June 2011, the number of days on which meteorological stations in Japan observed Kosa was 14, which was below the 1981 – 2010 normal of 23.1 (Figure 3, left). The total number of stations observing Kosa (referred to here simply as the total number of stations) over the same period was 220, which was near the normal of

212.7 (Figure 3, right).

The monthly total number of stations for May was 194 (normal: 32.9), which was the highest figure for the month since records began in 1967 (Figure 3, right). The main reason for this is that widespread Kosa moved over to Japan and many stations in the country observed it in the early part of the month.

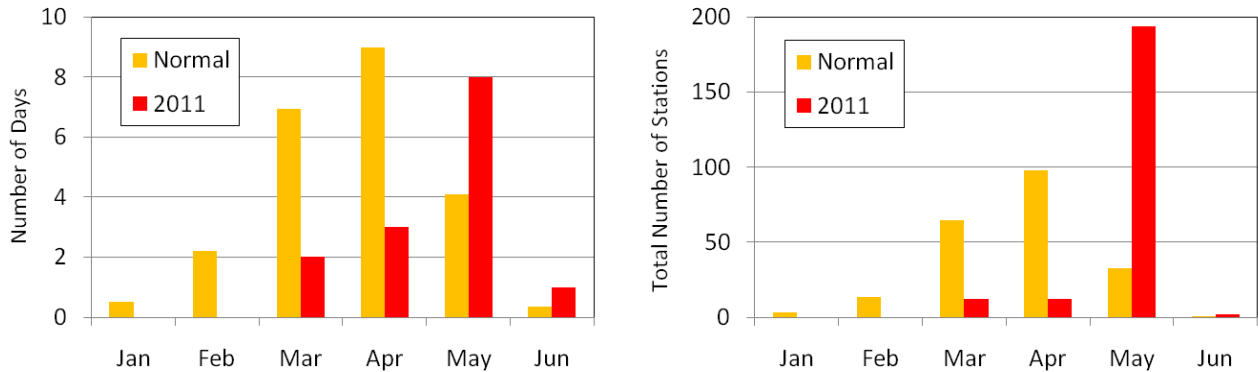


Figure 3 Monthly number of days when meteorological stations in Japan observed Kosa (left), and the monthly total number of stations observing Kosa (right) from January – June 2011

The red and yellow bars show the values for 2011 and the 1981 – 2010 normals, respectively.

Significant Kosa event in early May

Kosa was observed at many stations in western Japan, eastern Japan and Okinawa/Amami from 1 to 5 May. Minimum visibility of less than 5 km was observed at stations in Kyushu and elsewhere (Table 1). On 2 May, Kosa was observed at 43 out of 61 stations (Figure 4), which was the third-highest number for May and the eighth-highest for the year since records began in 1967. Although the Kosa event made the headlines on television and in newspapers, no flight cancellations or delays were reported.

JMA's Kosa prediction model forecasted this significant event, projecting that a large dust storm would arise around the Gobi Desert on 24 April, five days prior to the Kosa's

appearance (Figure 5). JMA closely monitored this area and confirmed surface observation reports of a dust storm with visibility levels of less than 2 km (Figure 6, left). The large dust storm around the Gobi Desert was also confirmed by analysis using MTSAT-2 satellite data (Figure 6, right). The Kosa prediction model forecasted that a dense mass of dust would move across North China and Korea and cover many areas of Japan. News reports detailed a dense dust storm over large areas of China and Korea, and JMA released information about the Kosa event to the public in order to call attention to it.

(Nozomu Ohkawara, Atmospheric Environment Division)

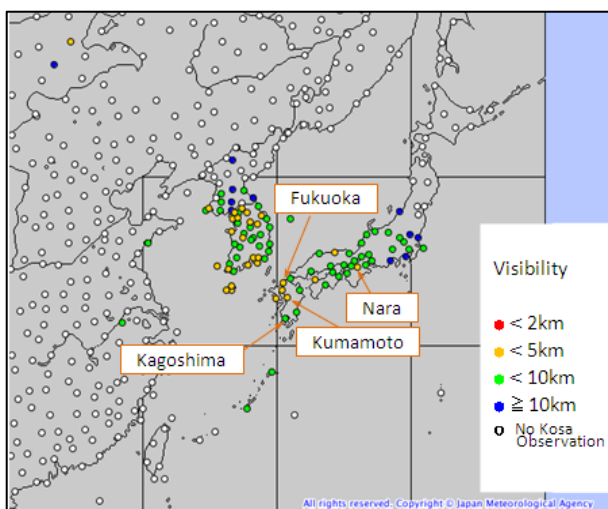


Figure 4 Meteorological stations observing Kosa and minimum visibility values for 2 May

Table 1 Daily number of stations observing Kosa and minimum visibility values recorded at stations from 1 to 5 May

Date	Number of Stations	Minimum Visibility (Station Name)
1 May	14	4 km (Fukuoka)
2 May	43	3 km (Kumamoto)
3 May	38	3 km (Kagoshima)
4 May	29	5 km (Nara)
5 May	16	10 km (Fukuoka, etc)

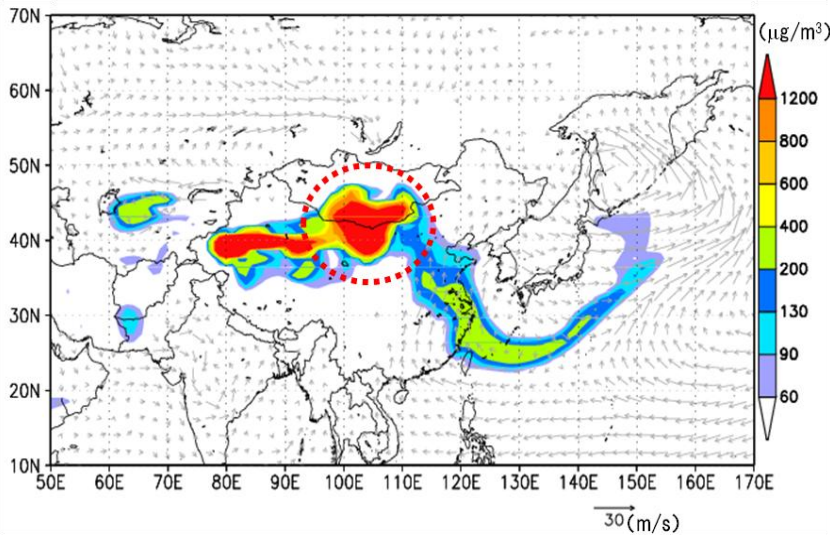


Figure 5 Forecast of surface dust concentration and surface wind by JMA's Kosa prediction model for 12 JST (03 UTC) on 29 April (initial time: 21 JST (12 UTC) on 24 April)
The red dashed circle shows a large dust storm around the Gobi Desert.

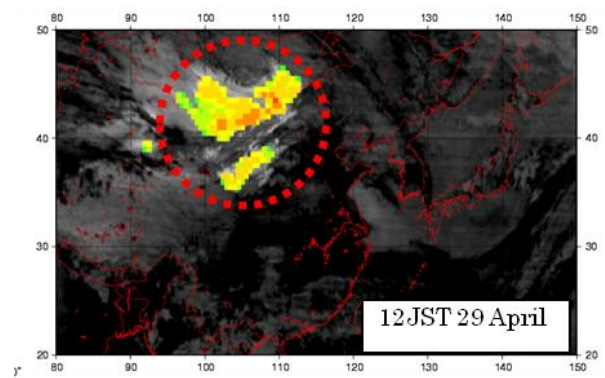
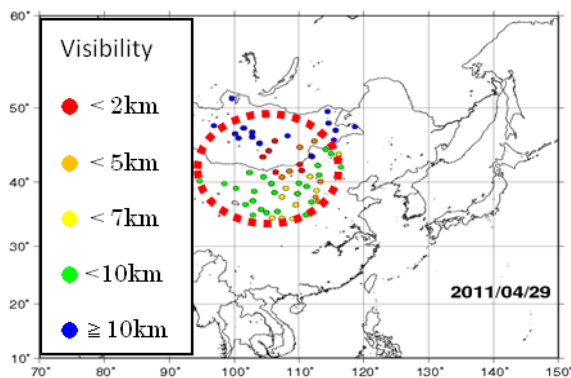


Figure 6 Meteorological stations in East Asia observing Kosa on 29 April (left) and the Kosa area analyzed from MTSAT-2 satellite data at 12 JST (03 UTC) on 29 April (right)
The red dashed circle in each figure denotes the area shown in Figure 5.

Sea Ice in the Sea of Okhotsk for the 2010/2011 Winter Season

The sea ice extent in the Sea of Okhotsk was smaller than normal for almost the whole of the 2011 sea ice season.

The sea ice extent in the Sea of Okhotsk was smaller than normal (i.e., the average for 1981 – 2010) for almost the whole of the 2011 sea ice season (from December 2010 to May 2011) (Figure 7). It reached its seasonal maximum of $94.54 \times 10^4 \text{ km}^2$ (below the normal of $116.92 \times 10^4 \text{ km}^2$) on 25 March (Figures 7 and 8). Figure 9 shows overall trends for the period from 1971 to 2011. Although the sea ice extent in the Sea of Okhotsk shows large interannual variations, there is a slight decreasing trend of $184 [70 - 298] \times 10^4 \text{ km}^2$ per decade (the numbers in square brackets indicate the two-sided 95% confidence interval) in the accumulated sea ice extent, and another slight decreasing trend of $6.0 [2.0 - 10.0] \times 10^4 \text{ km}^2$ (equivalent to 3.8% of the area of the Sea of Okhotsk) per decade in the maximum extent.

(Ryohei Okada, Office of Marine Prediction)

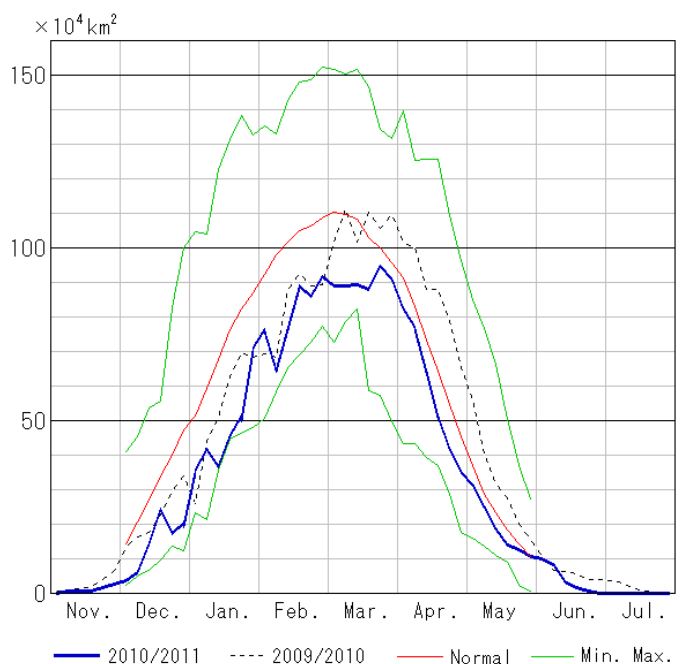


Figure 7 Seasonal variation of sea ice extent at five-day intervals in the Sea of Okhotsk from November 2010 to July 2011

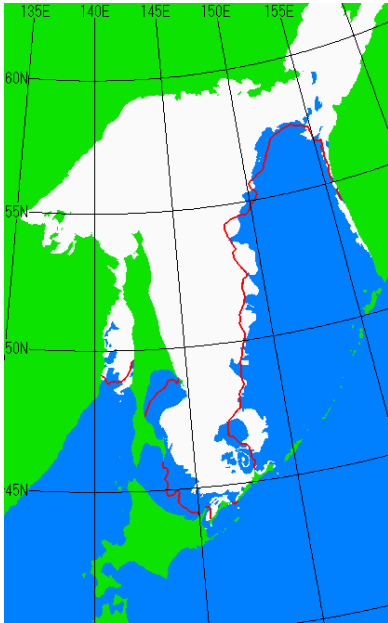


Figure 8 Sea ice situation on 25 March 2011

The white area shows the observed sea ice extent, and the red line indicates the extent of normal coverage (1981 – 2010).

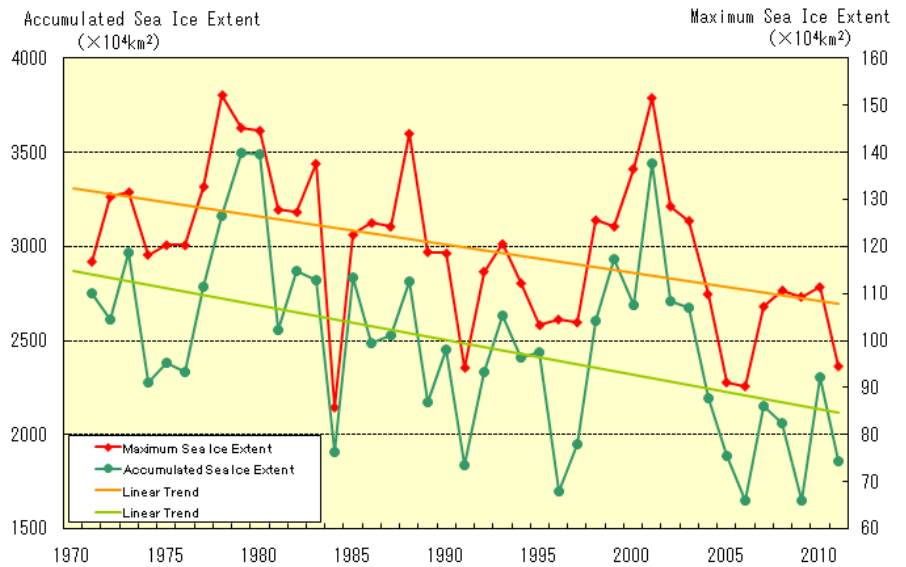


Figure 9 Interannual variations in the maximum sea ice extent (red line) and the accumulated sea ice extent (green line) in the Sea of Okhotsk from 1971 to 2011

Accumulated sea ice extent: the sum of all five-day sea ice extent values from December to May

JMA's New Climatological Normals for Atmospheric Circulation Fields

On 18 May, 2011, JMA updated its climatological normals to the 1981 – 2010 averages for operational use in climate system monitoring and climate prediction. This report briefly describes the present normals of atmospheric circulation fields and summarizes their characteristics compared to the previous normals (i.e., the 1979 – 2004 average). For details of other climatological normals including surface observation data and oceanographic data, see *TCC News No. 24 (Spring 2011)*.

The data used for monitoring and analyzing atmospheric circulation are global objective analysis figures from JMA's Climate Data Assimilation System (JCDAS), which is routinely operated and uses the same setup as that of the Japa-

nese 25-year reanalysis (JRA-25) (Onogi et al. 2007). The present atmospheric circulation normals are derived from the JRA/JCDAS data for the period from 1981 to 2010.

In the period from 2005 to 2010, which is included only in the present normals, there were three La Niña events and just one El Niño event. Conversely, neither El Niño nor La Niña events were seen in 1979 and 1980, which are included only in the previous normals. Accordingly, differences between the present and previous normals of atmospheric circulation indicate patterns seen in past La Niña events, particularly in the tropics (Figure 10).

Air temperatures for the lower and middle troposphere in the present normals are higher than those for the previous

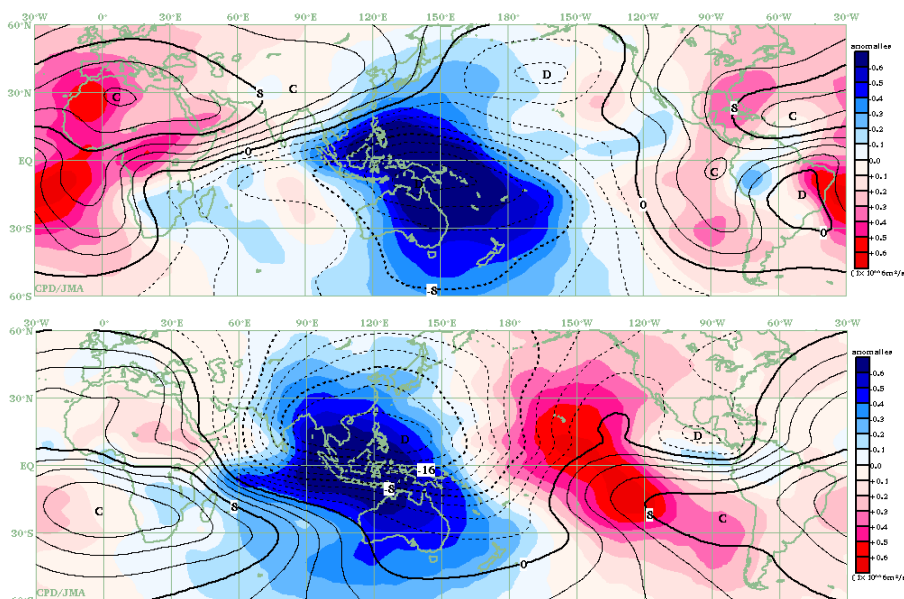


Figure 10 Differences between JMA's new and old normals for 200-hPa velocity potential (top: January; bottom: July)
The shading indicates deviations of 200-hPa velocity potential for the new normal from that for the old normal. The contours and vectors show 200-hPa velocity potential and divergent wind for the new normal, respectively.

normals (Figure 11). This may be associated with global warming and decadal-scale variability. It should be noted that air temperatures for the stratosphere in the present normals include a negative bias because such a bias is seen in JRA-25 stratospheric temperature data for the period between 1979 and 1998 (JMA 2007).

Reference

JMA, 2007: New climatological normals based on the JRA-25. *Monthly Report on Climate System Separated Volume No.13*, 139 pp.

Onogi, K., J. Tsutsui, H. Koide, M. Sakamoto, S. Kobayashi, H. Hatsushika, T. Matsumoto, N. Yamazaki, H. Kamahori, K. Takahashi, S. Kadokura, K. Wada, K. Kato, R. Oyama, T. Ose, N. Mannoji and R. Taira, 2007: The JRA-25 Reanalysis. *J. Meteor. Soc. Japan*, **85**, 369-432.

(Shotaro Tanaka and Hiroshi Ohno,
Climate Prediction Division)

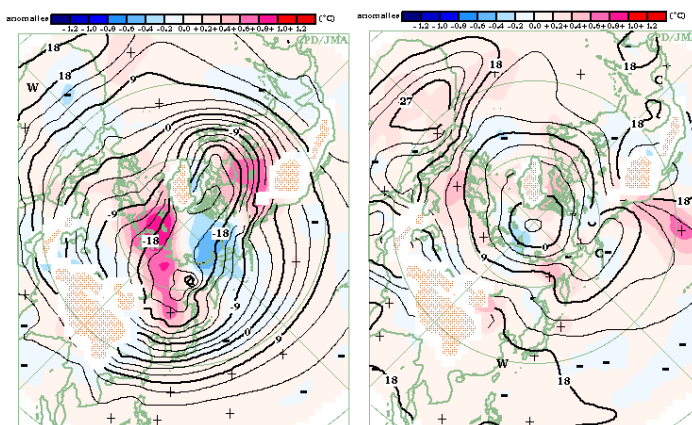


Figure 11 Differences between JMA's new and old normals of 850-hPa temperature (left: January; right: July)
The shading indicates deviations of 850-hPa temperature for the new normal from that for the old normal. The contours show 850-hPa temperature for the new normal.

The GFCS at the Sixteenth World Meteorological Congress

The Sixteenth World Meteorological Congress (Cg-XVI) was held in Geneva, Switzerland, from 16 May to 3 June, 2011, with the participation of more than 600 delegates, including senior government officials, heads of National Meteorological and Hydrological Services (NMHSs), and representatives of WMO partner organizations. One of the key issues at Cg-XVI was the establishment of the Global Framework on Climate Services (GFCS), which was proposed by the World Climate Conference-3 (WCC-3) (held in Geneva from 31 August to 4 September 2009) (see *TCC News No. 21 (Summer 2010)*). The congress decided that the framework would be one of the top five priorities of WMO over the next four years. The GFCS implementation plan will be developed by the WMO Executive Council for review and adoption at a 2012 extraordinary session of the World Meteorological Congress, which all relevant stakeholders (including UN bodies) are expected to attend.

In order to provide comprehensive and coherent information on the various components of the GFCS to congress delegates, a series of six interconnected side events on the theme of "The Role of NMHSs within the Global Framework for Climate Services (GFCS)" was organized. One of these events, entitled "Facilitating the Flow of Climate Information," introduced the coordinated Climate Services Information System (CSIS). This is a system to protect and distribute climate data and information according to the needs of users and according to the procedures agreed by governments and other data providers, and comprises global, regional and national centres and entities that generate/process climate information (Figure 12). This event was held on the evening of 20 May, 2011, and was moderated by Dr Richard Graham from the UK Met Office. As one of three lead speakers, TCC Head Ms Teruko Manabe gave a presentation on regional aspects of CSIS, including the activities of Regional Climate Centres (RCCs) and Regional Climate Outlook Forums (RCOFs).

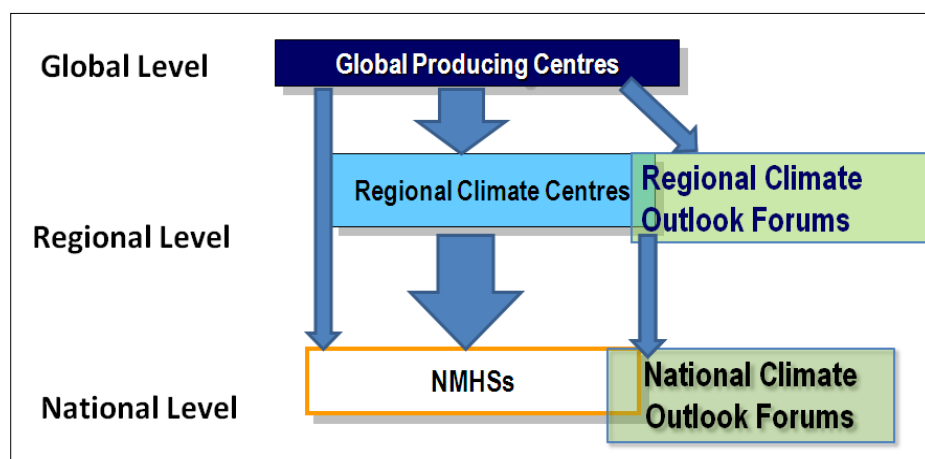
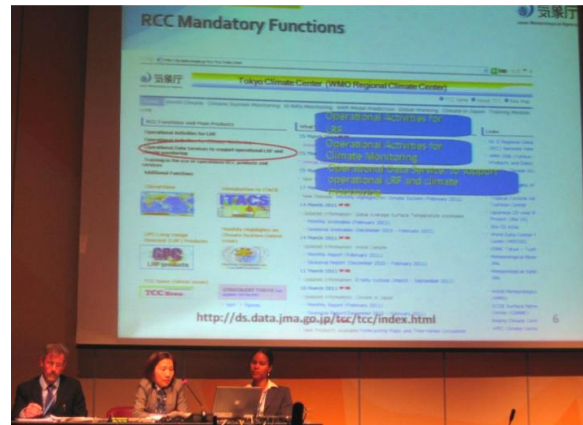


Figure 12
The three geographic domains (global, regional and national) and nodes in the CSIS

The congress recognized the important role of RCCs in tailoring global climate products to regional needs on a sustainable operational mode, and also in supporting national requirements of NMHSs where needed through mutual arrangements.

In accordance with the discussions held at Cg-XVI and the development of the GFCS, TCC will further enhance its activities to support climate services provided by NMHSs in the Asia-Pacific region.

*(Teruko Manabe, Tokyo Climate Center,
Climate Prediction Division)*



Introduction of New Services Available on the TCC Website

1. Addition of a new element (sea surface temperature) to the three-month probability forecast

TCC provides tercile probability forecasts for three-month-averaged temperature and precipitation. These forecasts are generated using the model output statistics (MOS) technique based on the 30-year hindcast.

In addition, the same forecast for sea surface temperature is now also produced (Figure 13). As with other forecasts, information on the level of forecast skill and verification data can be accessed by clicking any grid on the map. The forecast is normally updated around the 20th of every month, and is available at

<http://ds.data.jma.go.jp/tcc/tcc/products/model/probfcst/4mE/index.html>.

2. Warm/cold season probability forecasts and verification

TCC has started providing warm/cold season probability forecasts for temperature, precipitation and sea surface temperature (Figure 14). The warm season is the period from June to August, and the cold season runs from December to February.

The probability forecast as well as information on the level of forecast skill and verification data can be accessed by clicking any grid on the map.

The warm season probability forecast is issued in February, March and April, and the cold season forecast in September and October. The next forecast will be for the cold season from December 2011 to February 2012, and will be made available in September 2011 at <http://ds.data.jma.go.jp/tcc/tcc/products/model/probfcst/7mE/index.html>.

3. New provision of daily gridded data of one-month Forecasting

TCC starts providing daily gridded data (ensemble mean) of one-month forecasting in September 2011. The elements are almost equivalent for those of currently provided weekly data (ensemble mean), while daily spread and large anomaly index are not provided. The provision of weekly data (ensemble mean) will terminate in December 2011. More details are announced on the TCC website.

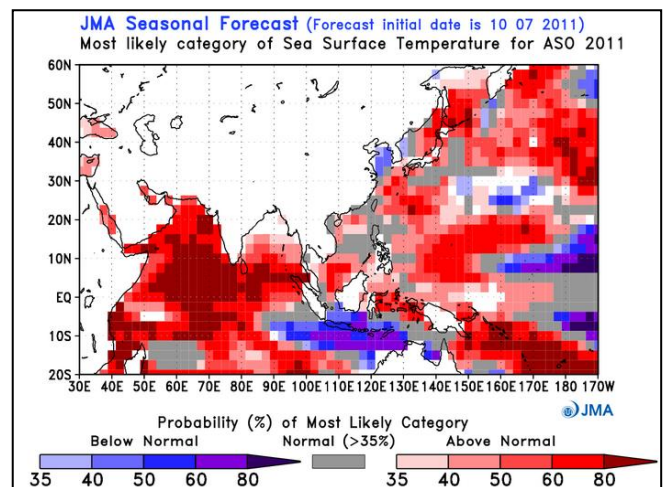


Figure 13 Three-month probability forecast of sea surface temperature for August – October 2011

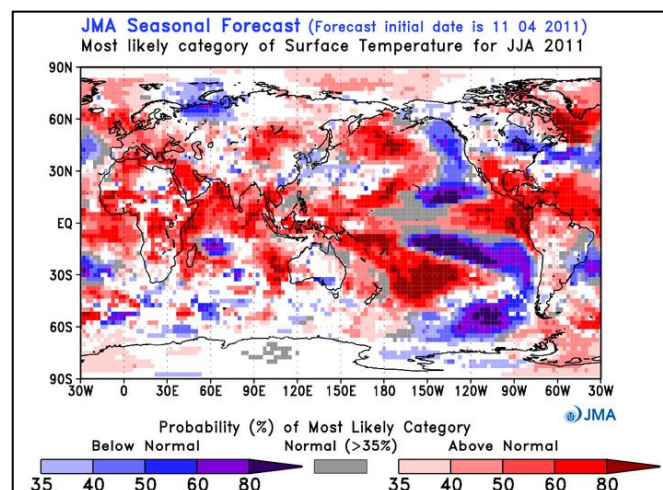
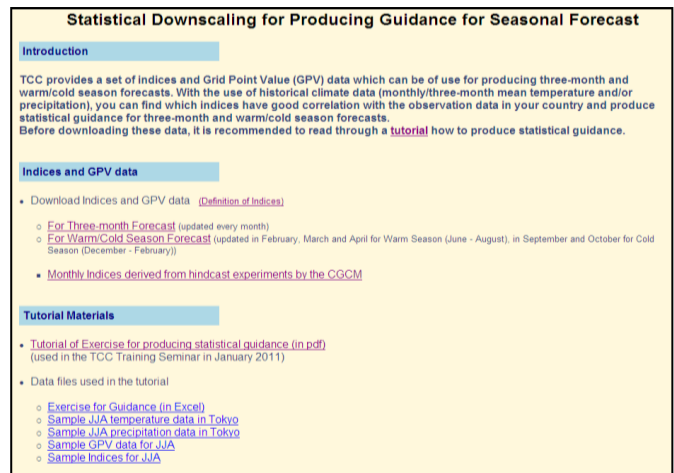


Figure 14 Warm season (June – August) probability forecast for temperature

4. New website on statistical downscaling for seasonal forecast guidance

TCC now provides a set of indices and gridded data that can be used to produce three-month and warm/cold season forecasts. From historical climate data (monthly/three-month mean temperature and/or precipitation), users can identify which indices show a close correlation to observation data in their countries and produce statistical guidance for three-month and warm/cold season forecasts. The site is open to registered NMHSs at <http://ds.data.jma.go.jp/tcc/tcc/gpv/indices/index.html>.

(Ryuji Yamada, Tokyo Climate Center,
Climate Prediction Division)



Top page of the statistical downscaling website

TCC and GPC Tokyo's Introduction as Operational DCPCs for the WMO Information System (WIS)

WMO has developed the WMO Information System (WIS) as a single coordinated global infrastructure responsible for telecommunications and data management functions. WIS consists of three types of centers: Global Information Service Centres (GISCs), Data Collection or Production Centres (DCPCs), and National Centres (NCs). In addition to enhancing the existing Global Telecommunication System, WIS provides data discovery, access and retrieval (DAR) services for all weather, climate, water and related data produced in the framework of any WMO programme. For this purpose, DCPCs maintain catalogues of their data and products, and provide appropriate parts of these catalogues to GISCs.

The Sixteenth World Meteorological Congress designated Tokyo as one of the GISCs in the WIS. The Tokyo Climate Center (TCC), the Global Producing Center of Long-range Forecasts (GPC) Tokyo and six other centers operated by JMA were also formally designated as DCPCs.

GISG Tokyo and the eight DCPCs are operational as

of 1 August, 2011. DAR services are expected to make products output by JMA's DCPCs (including TCC and GPC) more easily searchable and accessible by users.

For further information on WIS, GISG Tokyo and DCPCs, see the GISG Tokyo portal site at <http://www.wis-jma.go.jp/cms/>.



Top page of the GISG Tokyo portal site

New Head of the Tokyo Climate Center

Ms Teruko Manabe was appointed Head of the Tokyo Climate Center as of 1 April, 2011, succeeding Ms. Kumi Hayashi. Prior to joining TCC, Ms Manabe was the Head of the Office of Statistics in JMA. She has been

with the Agency for over 20 years, in which time she also worked in the WMO Secretariat for six years.

(Tokyo Climate Center)

Any comments or inquiry on this newsletter and/or the TCC website would be much appreciated. Please e-mail to: tcc@met.kishou.go.jp
(Editors: Teruko Manabe, Ryuji Yamada, Kenji Yoshida)

Tokyo Climate Center (TCC), Climate Prediction Division, JMA
Address: 1-3-4 Otemachi, Chiyoda-ku, Tokyo 100-8122, Japan
TCC Website: <http://ds.data.jma.go.jp/tcc/tcc/index.html>